Journal of Cardiology 62 (2013) 241–248

Contents lists available at ScienceDirect

Journal of Cardiology

journal homepage: www.elsevier.com/locate/jjcc

Original article

Identification and functional analysis of a novel PRKAG2 mutation responsible for Chinese PRKAG2 cardiac syndrome reveal an important role of non-CBS domains in regulating the AMPK pathway

Bi-li Zhang (MD)[1], Rong-liang Xu (MD)[1], Jing Zhang (MD), Xian-xian Zhao (MD), Hong Wu (MD), Li-ping Ma (MD), Jian-qiang Hu (MD), Jian-liang Zhang (MD), Zhong Ye (MD), Xing Zheng (MD)*, Yong-wen Qin (MD)*

Department of Cardiovascular Diseases, Changhai Hospital, Second Military Medical University, Shanghai 200433, China

ARTICLE INFO

Article history:
Received 9 August 2012
Received in revised form 28 February 2013
Accepted 12 April 2013
Available online 15 June 2013

Keywords:
PRKAG2
AMPK
Gene mutation
Familial cardiac syndrome
CBS

ABSTRACT

Background: PRKAG2 gene encodes the γ_2 regulatory subunit of AMP-activated protein kinase (AMPK) that acts as a sensor of cellular energy status, and its germline mutations are responsible for PRKAG2 cardiac syndrome (PCS). The majority of missense mutations of cystathionine beta-synthase (CBS) domains found in PCS impair the binding activity of PRKAG2 to adenosine derivatives, and therefore lead to PRKAG2 function impairment and AMPK activity alteration, resulting in a familial syndrome of ventricular preexcitation, conduction defects, and cardiac hypertrophy. However, it is unclear about the PRKAG2 mutation in the non-CBS domain. Here, a Chinese family exhibiting the cardiac syndrome associated with a novel heterozygous PRKAG2 mutation (Gly100Ser) mapped to exon 3 encoding a non-CBS domain is described and the function of this novel mutation was investigated *in vitro*.

Methods: The PRKAG2 G100S and R302Q mutations were constructed by a two-step polymerase chain reaction and then transfected into CCL13 cells by lentivirus vectors. Wild-type PRKAG2 gene transfection was used as a negative control. PRKAG2 expression was determined by Western blot. Immunofluorescence was used to localize the intracellular PRKAG2 proteins. MTT assay was performed to explore the effect of mutations on cell proliferation. Periodic acid-Schiff staining was used for detecting glycogen accumulation. AMPK concentration was measured with enzyme-linked immunosorbent assay.

Results: Our results showed neither intracellular localization of PRKAG2 nor cell growth was altered. In contrast, PRKAG2 protein expression levels were significantly reduced by this mutation. Furthermore, PRKAG2-mediated activity of AMPK was attenuated, resulting in glycogen metabolism dysregulation. These findings revealed that non-CBS domains of PRKAG2 were essential to the regulation of AMPK activity, similar to CBS.

Conclusions: Our study ascribes a crucial regulatory role to the novel PRKAG2 G100S mutation, and reiterates that PCS occurs as a consequence of AMPK signaling abnormality caused by PRKAG2 gene mutations.

Introduction

PRKAG2 cardiac syndrome (PCS) is a relatively rare autosomal dominant genetic disease of the heart, typified by familial cardiac genetic disease or sporadic cases. PCS patients are predisposed to the development of various cardiac clinical changes such as ventricular preexcitation, progressive conduction system disease, ventricular hypertrophy, and even sudden death as well as muscular and skeletal lesions. Germline mutations in the PRKAG2 gene, which encodes the γ2 subunit of AMP-activated protein kinase (AMPK) and is located on chromosome 7p36.1, have been identified in the majority of PCS patients. AMPK, a heterotrimeric protein kinase composed of a catalytic subunit (α) and two regulatory subunits (β and γ), acts as a sensor of cellular energy status and is activated under conditions of energy depletion manifested by increased cellular AMP levels [1]. Dominant mutations of PRKAG2 seldom occur in sporadic cases but appear relatively common in family constellation. Identification of PRKAG2 mutations in

* Corresponding authors at: Department of Cardiovascular Diseases, Changhai Hospital, Second Military Medical University, 168 Changhai Road, Shanghai 200433, China. Tel.: +86 21 3116 1255; fax: +86 21 3116 1248.
E-mail address: zhengxing57530@163.com (X. Zheng).
[1] Co-first authors.

0914-5087/$ – see front matter © 2013 Japanese College of Cardiology. Published by Elsevier Ltd. All rights reserved.
http://dx.doi.org/10.1016/j.jjcc.2013.04.010

families coupled with their functional analysis supports the notion that mutational PRKAG2 is a cause of PCS. Mutations recognized thus far include His142Arg, Arg302Gln, His383Arg, Thr400Asn, Tyr487His, Asn488Ile, Gln506Lys, Arg531Gly, Ser548Pro, and InsLeu351 [2–10]. These mutations invariably cluster within the Bateman domain [the region defined as the cystathionine beta-synthase (CBS) domains] of the PRKAG2 gene. The mutation Arg302Gln is most common among them in clinical isolates.

Studies in both cellular and murine models of PRKAG2 cardiac syndrome have successfully demonstrated that PRKAG2-mediated cardiomyopathy is a distinct type of glycogen storage disease involving primarily the heart. Consistent with a causative role of PRKAG2 in PCS, heterozygous mice carrying a mutant PRKAG2 allele develop pathological cardiac changes resembling the human genetic disorder. Several *in vitro* and *in vivo* studies suggest that PCS is caused by increased AMPK activity [5,11]. Paradoxically, introduction of several PRKAG2 mutants into mammalian CCL13 cells or over-expression of Arg302Gln and Arg531Gly mutations in transgenic mouse models can lead to a decrease or no change in AMPK activity [12–15]. Furthermore, a study by Banerjee et al. shows that the PRKAG2 Thr400Asn mutation results in early activation of myocardial AMPK, followed by depression, and then recovery to wild-type levels [16]. Taken together, the above-mentioned studies support the notion that dysregulation of AMPK activity (either activating or inhibiting) contributes to the development of PCS. However, these studies are far from revealing the full functional capacity of PRKAG2.

In the current study, we were surprised to find a Chinese family with a new missense mutation (Gly100Ser) in PRKAG2 gene. Associated with this mutation, the family manifests ventricular preexcitation, severe conduction system abnormalities, and cardiac hypertrophy, similar to Western families in phenotype. Interestingly, this mutation is located in a non-CBS domain, different from all previously characterized mutations. We further show that the mutation can result in excessive glycogen accumulation in cell models by expressing this mutant PRKAG2 gene, which can be attributed to reduced PRKAG2 protein expression and PRKAG2-mediated activity of AMPK. Thus, these results reveal a novel role of the non-CBS domain of PRKAG2 in the regulation of AMPK activity, and link the mutation in non-CBS domains to PCS for the first time in a challenge to the dogma that gene mutations in CBS domains are responsible for familial PRKAG2-mediated cardiomyopathy. The study provides the basis for further elucidation of the molecular network that leads to development of PCS in the Chinese population.

Materials and methods

Study cohort

A Chinese family with ventricular preexcitation accompanied with conduction abnormity and cardiac hypertrophy was investigated. Another simple hypertrophic cardiomyopathy family and 100 unrelated healthy individuals were studied as controls. Informed consent was obtained from study participants. Family members were evaluated by a detailed history, physical examination, 12-lead electrocardiogram (ECG), ultrasound cardiogram, and dynamic ECG. The information on dead familial members was obtained by history-taking and consulting medical records. The diagnosis of ventricular preexcitation was made on the basis of a short PR interval (<120 ms), widened QRS interval (>110 ms), and abnormal initial QRS vector (δ wave). Moreover, the diagnosis of conduction system disease was ascertained owing to evidence of sinus node dysfunction or atrioventricular block on ECG, as described previously [3]. Cardiac hypertrophy was diagnosed on the basis of incrassate interventricular septum or ventricular wall, according to diagnostic criteria of hypertrophic cardiomyopathy [17–19]. Clinical features of the family were summarized and pedigree of family was drawn using Cyrillic 2.02 software. In addition, serum creatine kinase levels of study participants were determined by automatic biochemical analyzer.

Mutation analysis

Blood was collected from each study individual and DNA was extracted using Flexi Gene DNA kit (QIAGEN, Hilden, Germany). The genomic structure and cDNA sequence of PRKAG2 were obtained from the GenBank database (accession number: NM_016203) and oligonucleotide primers were designed for exons 1–16. Amplifications of 16 exons were performed by polymerase chain reaction (PCR). The products of each PCR reaction were checked on 1.5% sepharose and purified using the QIAquick PCR purification kit (QIAGEN). Direct sequencing reactions in both the sense and antisense direction were performed on an ABI377 automatic sequencer (Applied Biosystems, Foster City, CA, USA). Sequences were compared with published genomic sequences of the PRKAG2 gene.

Construction of plasmids and expression in CCL13

The incomplete PRKAG2 cDNA clone (GenBank accession number BC068598), which presents N-end loss of 44 amino acids, was obtained by purchase. The PRKAG2 gene sequence was designed according to the known PRKAG2 gene sequence (GenBank accession number NM_016203). The full-length PRKAG2 gene was acquired using the designed primers by PCR-based gene assembly method. The PCR product was cloned into TA cloning vector. To introduce the G100S and R302Qmutations (designated GS and RQ) into PRKAG2, a two-step polymerase chain reaction method was used. PCR products (GS and RQ) and TA cloning vector containing wild-type PRKAG2 gene (WT) were digested with MluI and NdeI and subcloned into the lentivirus vector. The CCL13 cells (provided by Dr. Hua-mao Wang, University of Fudan) were cultured in Dulbecco's modified Eagle's medium (DMEM) containing 10% (v/v) fetal bovine serum. After being cultured for 24 h, CCL13 cells were infected with LV-GS, LV-RQ, and LV-WT at a MOI of 10. After transfection, CCL13 cells stably expressing either G100S AMPK-γ2, R302Q AMPK-γ2, or WT were cultured as above. The expression of AMPK-γ2 was checked by Western blotting using anti-γ2 antibodies.

Western blot analysis

Immunoblotting was performed to detect the expression of PRKAG2 in CCL13 cell lines infected by recombinant lentivirus. CCL13/LV-WT, CCL13/LV-GS, and CCL13/LV-RQ cells were scraped off and harvested. All cells were lysed in RIPA buffer [50 mM TrisC1, 50 mM NaCl, 10% glycerol, 1% Nonidet P-40, 0.5% deoxycholate, 0.1% sodium dodecyl sulfate (SDS), 10 mM NaF, 0.4 mM ethylene diamine tetraacetic acid (EDTA), pH 8.0, with leupeptin and aprotinin] and centrifuged at 12,000 × g for 10 minutes. Samples with 50 μg of total protein were resolved by SDS-polyacrylamide gel electrophoresis (SDS-PAGE) on a 10% gel and transferred onto a nitrocellulose (NC) membrane. The blot was incubated with Tris buffered saline with Tween (TBST) with 1:200 rabbit primary antibody against human PRKAG2 (ProteinTech Group, Inc., Chicago, IL, USA), followed by the secondary horseradish peroxidase (HRP)-conjugated anti-rabbit antibody (Santa Cruz Biotechnology Inc., Dallas, TX, USA). After washing, the bands were detected by enhanced chemiluminescence (ECL) detection kit and imaged with a Kodak film (Rochester, NY, USA). Glyceraldehyde-3-phosphate dehydrogenase (GAPDH) was used as an endogenous protein for normalization.

Immunofluorescent cytochemistry

The 4% paraformaldehyde-fixed cells were examined for the presence of WT or mutant PRKAG2. Slides with cultured CCL13/LV-WT, CCL13/LV-GS, and CCL13/LV-RQ cells were incubated for 1 h at room temperature in blocking buffer that contained 1% bovine serum albumin (BSA) and 0.1% Triton X-100 in phosphate buffered solution (PBS). The cells were then incubated with rabbit anti human PRKAG2 poly antibody as primary antibodies (Protein-Tech) in PBS for 2 h at room temperature. Tetramethylrhodamine isothiocyanate-conjugated anti-rabbit IgG was diluted 1:500 in PBS and used as the secondary antibody (KPL, Guildford, UK) incubated for 30 minutes at room temperature. Slides and coverslips were washed three times in PBS, after which the cells were viewed by fluorescence microscope (Eclipse E 800; Nikon, Tokyo, Japan) and imaged with a Kodak film.

Enzyme-linked immunosorbent assay for AMPK concentration

CCL13/LV-WT, CCL13/LV-GS, and CCL13/LV-RQ cells were seeded to 6-well microtiter plates at 2×10^5 cells/well and incubated at 37 °C with 5% CO_2 for 24 h. The media containing the AMPK activator 5-aminoimidazole-4-carboxamide-1-β-d-ribofuranoside (AICAR) of two concentrations (0.5 mM, or 2 mM) was exchanged to each well 60 min before the end of incubation, respectively. After various treatments, cells were lysed *in situ* using 0.3 ml of ice-cold lysis buffer [50 mM Tris/HCl (pH 7.2), 1 mM ethylene glycol tetraacetic acid (EGTA), 1 mM EDTA, 50 mM NaF, 1 mM Na pyrophosphate, 1% [w/v] Triton X-100, 0.1 mM phenylmethane sulphonyl fluoride (PMSF), 1 mM dithiothreitol (DTT), 0.1 mM benzamidine, and 5 μg/ml soybean trypsin inhibitor]. The lysates were centrifuged (4 °C, 10 min, 21,000 × g) and the supernatants were collected for AMPK enzyme-linked immunosorbent assay (ELISA). The concentrations of AMPK in supernatants were determined by ELISA kit according to the manufacturer's instructions (ADL, Washington, USA). Briefly, these assays employed the quantitative sandwich enzyme immunoassay technique with biotinylated monoclonal antibodies specific for AMPK. Standard controls and samples (100 mL of supernatant) and biotinylated monoclonal antibodies were simultaneously pipetted into the wells in triplicate and incubated for 1 h at 37 °C. After AMPK binding and washing, the enzyme (streptavidin-peroxydase) was added to each well. After incubation and thorough washing to remove all unbound enzyme, a substrate solution which was acting on the bound enzyme was added to induce a colored reaction product. The intensity of this colored product is directly proportional to the concentration of AMPK present in the samples. The optical density of each well was determined by a microplate reader at 450 nm.

Periodic acid-Schiff staining for glycogen

Sterile slides were put into 24-well microtiter plates, one in each well. Then, CCL13/LV-WT, CCL13/LV-GS, and CCL13/LV-RQ cells were digested, counted and seeded to slides at 1×10^4 cells/well. To be covered with 70% of cells, cells were deprived of serum for 12 h and then incubated with 1640 medium at 37 °C with 5% CO_2 for 24 h. Accumulated glycogen was measured after slides containing cells were fixed in 4% formaldehyde with 1% periodic acid and Schiff's (PAS) reagent (Sigma, St Louis, MO, USA) as described previously [20].

MTT assay for CCL13 cell proliferation

CCL13/LV-WT, CCL13/LV-GS, and CCL13/LV-RQ cells were deprived of serum for 12 h and then exposed to the same concentration of AICAR (0.5 mmol/L) for 30 min, 90 min, and 24 h, respectively. Proliferation was then determined in triplicate with a colorimetric nonradioactive, MTT proliferation assay. After exposure of CCL13 cells of every group to AICAR, 10 μl MTT reagent [3-(4,5-dimethylthiazol-2-yl)-2,5-diphenyltetrazolium bromide, 5 mg/ml in PBS; Sigma] was added and allowed to incubate at 37 °C for 4 h. After the incubation, samples were placed in a microtiter plate and the absorbance was read at 450 nm with an ELISA plate reader.

Statistical analysis

Data are expressed as the mean ± standard deviation (SD). Student's *t*-test for paired values was used to analyze data. *p*-Values less than 0.05 were regarded as statistically significant. All of the analyses were performed using SPSS for Windows (version 10.0; SPSS Inc., Chicago, IL, USA).

Results

Clinical characteristics of patients

A 4-generation family with 12 affected individuals diagnosed as having Wolff–Parkinson–White syndrome, conduction system disease, and/or hypertrophic cardiomyopathy was studied (Fig. 1 and Table 1). Clinical presentation of symptomatic arrhythmias of affected family members (7 males and 5 females) occurred from age 16 to 41 years. Eight had asymmetrical ventricular septal hypertrophy with mean thickness 2.09 ± 0.98 cm and cardiac hypertrophy did not cause left ventricular outflow tract obstruction (Fig. 2A and B). Eight had atrioventricular block or sinus abnormality requiring permanent pacemaker implantation. Six had ventricular preexcitation and 3 of them showed short PR interval on ECG (Fig. 2C). Five had superventricular tachycardia (4 atrial fibrillation and 1 atrial tachycardia). Four showed cardiac dilation and heart failure at the terminal stage of disease and 1 died suddenly when young. Serum creatine kinase levels were normal in all affected family members.

Identification of a novel PRKAG2 mutation

A previously undetected missense mutation, glycine (100) to serine, in exon 3 of PRKAG2 was identified and shown to be present in 7 living affected individuals who were more than 25 years old and 2 family members of the fourth generation who were less than 25 years old and asymptomatic (Fig. 3A). The mutation results from guanine (G) substituted by adenine (A) at nucleotide

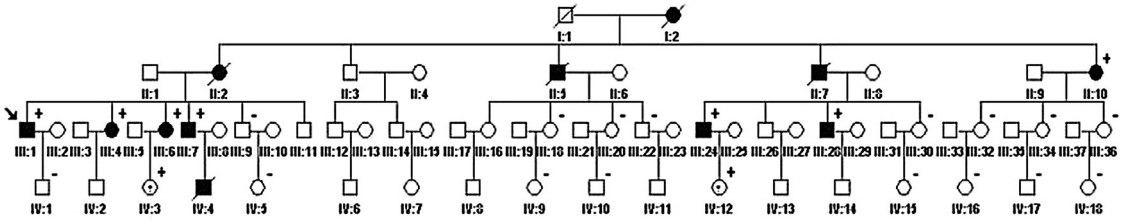

Fig. 1. Pedigree of a Chinese PRKAG2 cardiac syndrome family. Squares indicate males, and circles, females. Affected individuals are represented by solid symbols.

Table 1
Clinical features of family members with PRKAG2 mutation.

Case	Sex	Age of onset (years)	ECG/HOLTER	UCG	Therapy/prognosis
II:2	F	–	Sinus bradycardia, Morse I type AVB, CRBBB	IVS 2.8 cm EF 40.1%	Symptomatic treatment, deceased
II:5	M	35	Sinus bradycardia, III° AVB, WPW, paroxysmal atrial tachycardia	IVS 2.28 cm EF 56.4%	PPM, deceased
II:7	M	–	–	–	PPM, deceased
II:10	F	38	Sinus bradycardia, sinus bradycardia, short PR interval, Morse I type AVB, AF	IVS 1.3 cm	Untreated
III:1(proband)	M	34	Sinus bradycardia, Morse II type AVB, AF	IVS 3.2 cm EF 28.7%	PPM
III:4	F	24	Sinus bradycardia, sinus bradycardia, short PR interval, CRBBB,AF	IVS 1.3 cm	PPM
III:6	F	41	Sinus bradycardia, sinus bradycardia, short PR interval, paroxysmal atrial tachycardia, AF, intermittency intra-atrial block	IVS 1.3 cm	Symptomatic treatment
III:7	M	28	Sinus bradycardia, WPW, paroxysmal tachycardia	IVS 2.26 cm	Untreated
III:24	M	33	Sinus bradycardia, atrial premature	Normal	Symptomatic treatment
III:28	M	26	Sinus bradycardia, CRBBB	Normal	–
IV:3	F	16	Sinus rhythm, IRBBB	Normal	–
IV:4	M	18	WPW	IVS 1.9 cm	Sudden death at 21
IV:12	F	–	Sinus arrhythmia, IRBBB	Normal	–

ECG, electrocardiogram; AVB, atrio-ventricular block; WPW, Wolff–Parkinson–White syndrome; AF, atrial fibrillation; CRBBB, complete right bundle branch block; IRBBB, incomplete right bundle branch block; EF, ejection fraction; PPM, permanent pacemaker; IVS, interventricularseptal thickness.

298 (Fig. 3B). Direct DNA sequencing of a simple hypertrophic cardiomyopathy family and 100 unrelated healthy individuals did not show this mutation. The evolutionary conservation of PRKAG2 Gly100 residue between fish and humans is shown in Fig. 3C.

Intracellular localization of mutant PRKAG2 proteins

To explore the effects of G100S mutation in non-CBS of PRKAG2, we first examined whether and where mutant PRKAG2 proteins were expressed in CCL13 cells by transfecting the PRKAG2 cDNAs into CCL13 cells. The most common mutation (R302Q) in CBS was used as a positive control. Western blot analysis using whole cell lysates revealed that two mutants and WT were expressed in CCL13 cells at comparable levels (Fig. 4). Immunocytochemistry using anti-PRKAG2 antibody revealed that transfected WT, RQ, and GS were diffusely localized in both the cytoplasm and nucleus of CCL13 cells (Fig. 5).

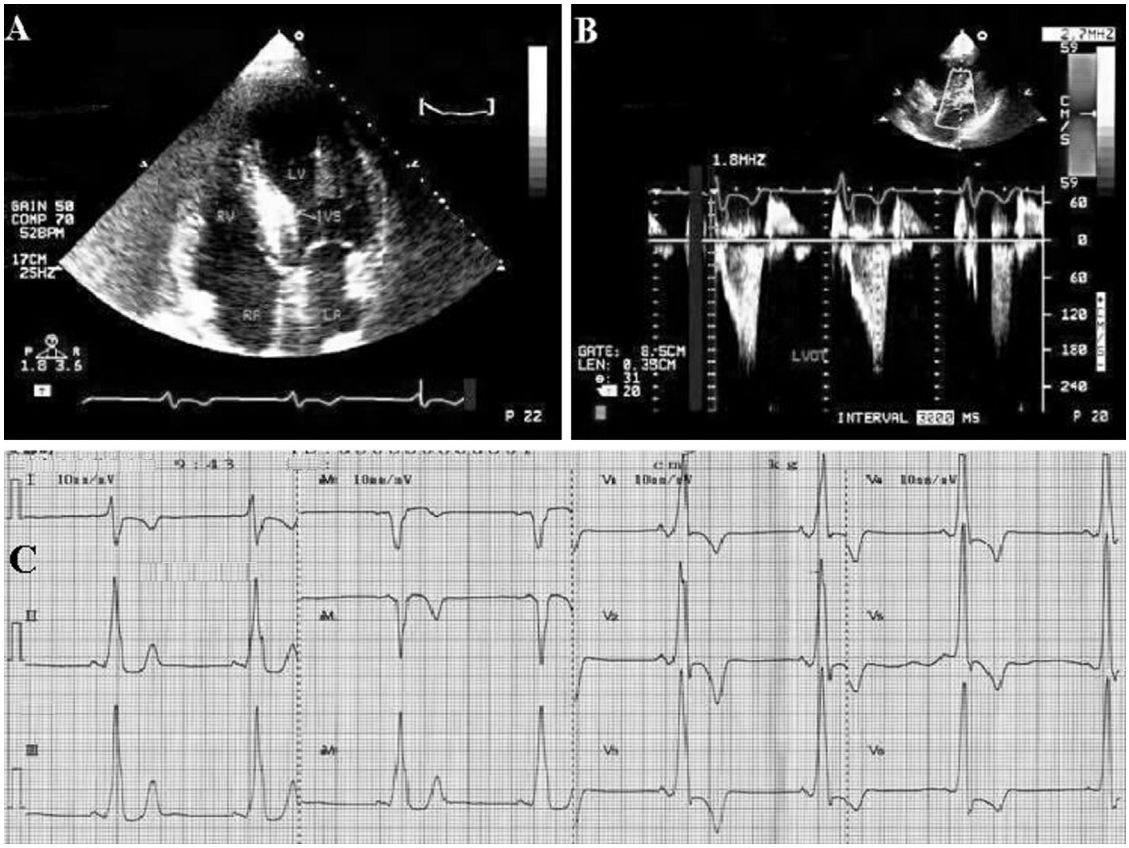

Fig. 2. (A) Echocardiographic apical four-chamber view demonstrates a normal posterior wall and septal hypertrophy. (B) Ultrasonic spectrum shows left ventricular outflow tract pressure gradient is 18 mmHg. (C) Archived electrocardiogram of the proband demonstrates ventricular preexcitation.

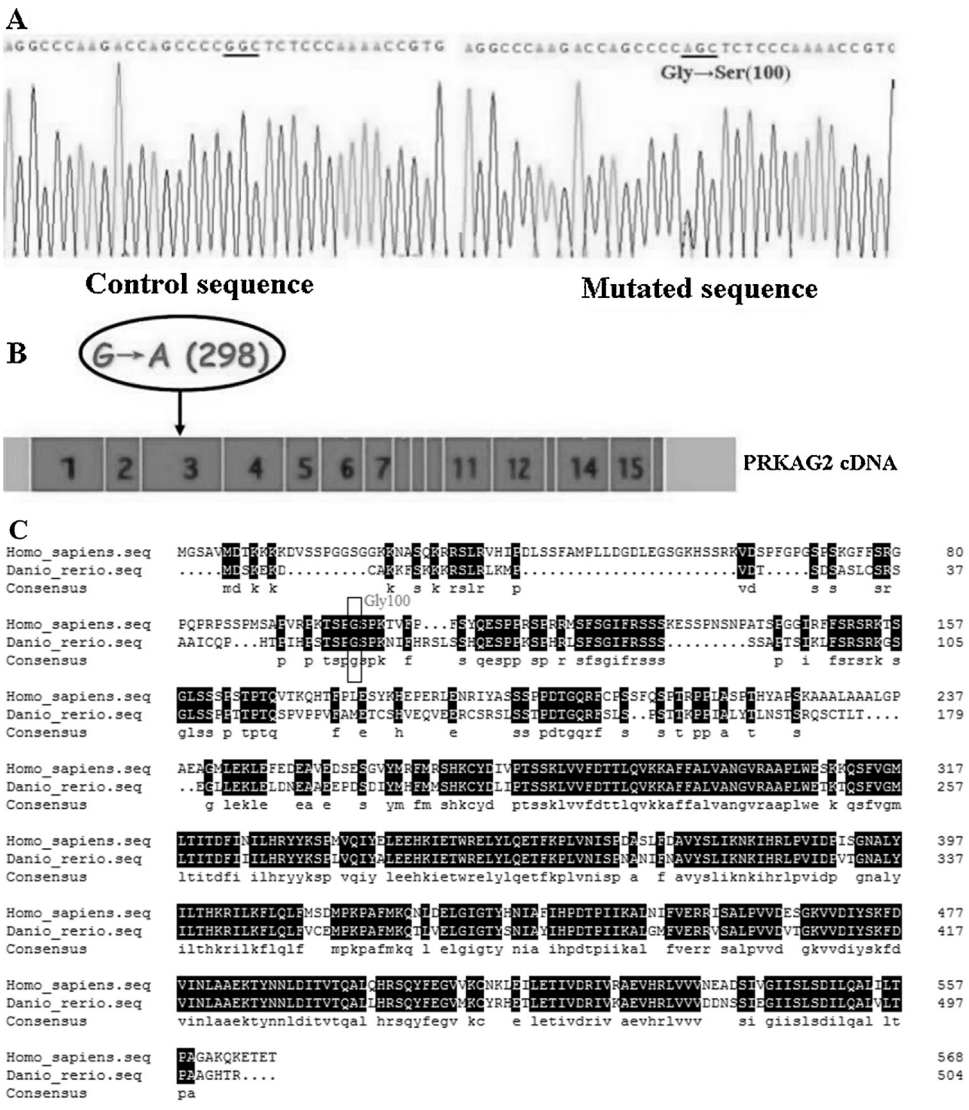

Fig. 3. PRKAG2 mutation in affected patients detected by DNA sequencing. (A) Sequencing analysis showed a Gly100Ser amino acid substitution in the protein product. (B) Sequence data from PRKAG2 exon 3 showing a heterozygous G→A transition at nucleotide 298. Arrow heads mark the site of the base alteration. (C) The evolutionary conservation of PRKAG2 Gly100 residue between fish (accession number: XP_696730.3) and human (accession number: NP_057287.2), which was constructed by using the DANMAN7.0.

Reduction in AMPK concentration in PRKGA2 mutant-expressing cells

AMPK is an important protein kinase found in all eukaryotic cells. AMPK concentrations of CCL13/WT, CCL13/GS, and CCL13/RQ cells were measured by ELISA after adding AICAR at two concentrations. AMPK concentration was significantly elevated corresponding to increased AICAR concentrations in all groups (Fig. 6). With or without AICAR, AMPK concentrations of CCL13/GS and CCL13/RQ cells were significantly decreased compared to that of CCL13/WT cells. In addition, CCL13/GS cells exhibited a significant difference in AMPK concentration compared with CCL13/RQ cells. These findings indicate that AMPK concentration can represent AMPK activity to a suitable degree. Moreover, PRKAG2 G100S and R302Q degraded the AMPK activity of CCL13 cells, whereas the influence of PRKAG2 G100S to AMPK activity was less than that of PRKAG2 R302Q.

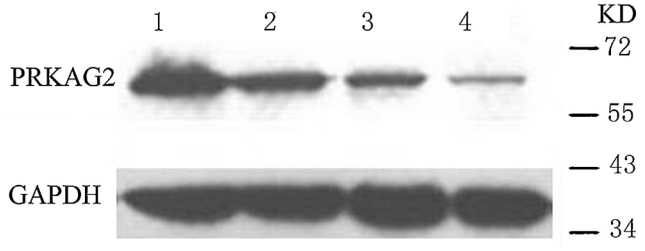

Fig. 4. Western blot analyses using antibody specific for PRKAG2 reacted with whole cell lysates from PRKAG2-transfected and non-transfected CCL13 cells. The PRKAG2 protein is of 63 kDa. GAPDH serves as a loading control. Lane 1, CCL13/WT; lane 2, CCL13/GS; lane 3, CCL13/RQ; lane 4, non-TG CCL13.

Accumulation of glycogen in PRKGA2 mutant-expressing cells

Previous studies have reported that some missense mutations (N488I, R302Q, R531G, and T400N) in CBS of the PRKAG2 gene cause a marked accumulation of cardiac glycogen [5,11,14–16]. To determine whether the PRKAG2 mutation in non-CBS results in glycogen accumulation, CCL13/WT, CCL13/GS, and CCL13/RQ cells were analyzed by staining them with PAS reagent. Increased glycogen accumulation was detected in CCL13/GS and CCL13/RQ cells, compared to CCL13/WT cells (Fig. 7).

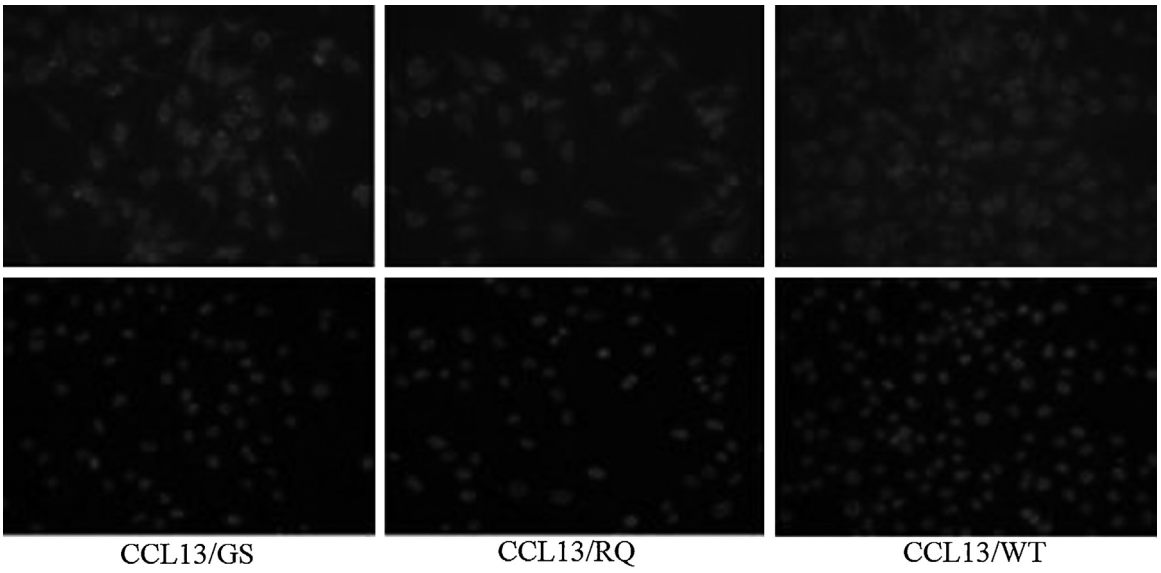

Fig. 5. Immunocytochemistry using anti-PRKAG2 antibody revealed that transfected WT, RQ, and GS are diffusely localized in the cytoplasm and nucleus of transfected CCL13 cells.

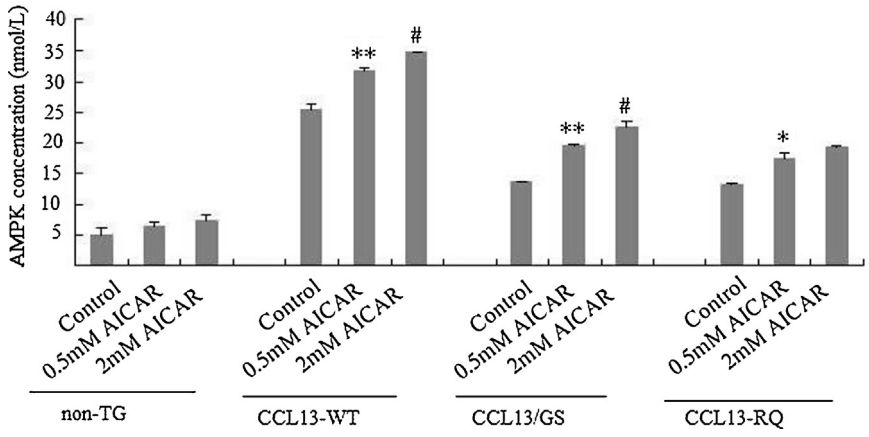

Fig. 6. Non-5-aminoimidazole-4-carboxamide-1-β-D-ribofuranoside (AICAR)-stimulated and AICAR-stimulated AMP-activated protein kinase (AMPK) levels in CCL13 cells. AMPK concentration was measured by enzyme-linked immunosorbent assay after adding AICAR at two concentrations. AICAR induces a dose-dependent increase in AMPK concentration at 60 min. Data are expressed as mean ± SEM of three experiments. $^{*}p < 0.05$, $^{**}p < 0.01$ *vs.* control levels; $^{\#}p < 0.05$ *vs.* 0.5 mM AICAR group.

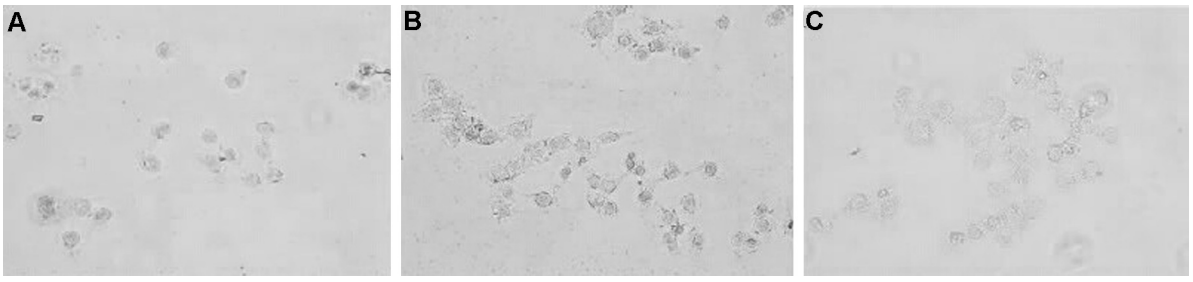

Fig. 7. Periodic acid-Schiff (PAS) staining of every group of CCL13 cells. (A) CCL13/GS cells; (B) CCL13/RQ cells; and (C) CCL13/WT cells. Scale bar = 200 μm.

Proliferation of CCL13 cells in response to PRKAG2 mutations

Next, we sought to determine whether gene mutations can influence CCL13 cell proliferation following addition of AICAR. The results showed AICAR did not elicit mutation-related increase or decrease in CCL13 cell proliferation after 30 min, 90 min, and 24 h (Fig. 8).

Discussion

In this study, we describe a Chinese family with a new heterozygous PRKAG2 mutation (G100S) mapped to exon 3, which manifests ventricular preexcitation, severe conduction system abnormalities, and cardiac hypertrophy. Moreover, we also introduce a cell model of PRKAG2 cardiac syndrome caused by the G100S mutation. Our

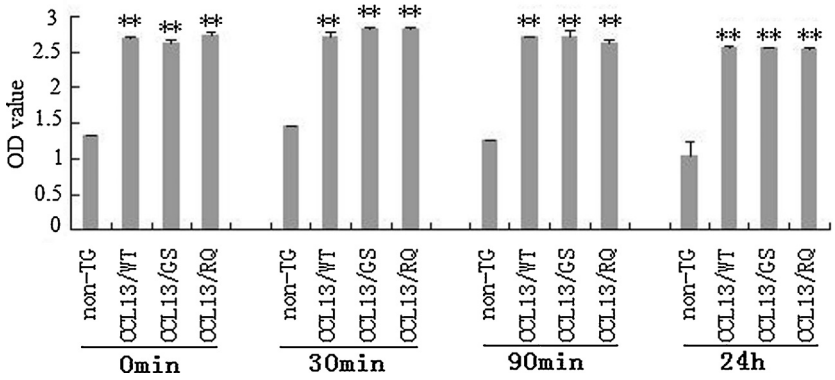

Fig. 8. Impact of mutation on cell proliferation after 5-aminoimidazole-4-carboxamide-1-β-d-ribofuranoside (AICAR) treatment. 0.5 mM AICAR did not induce mutation-related increase or decrease in CCL13 cell proliferation at all the time points. Values are expressed as mean ± SEM of three experiments. $^{**}p < 0.01$ *vs.* non-TG group.

studies in both humans and cells provide strong evidence for the role of PRKAG2 in the physiology of heart and the pathogenesis of PCS, a relatively rare autosomal dominant disorder. Multiple lines of evidence indicate that the G100S mutation in PRKAG2 on chromosome 7p36 results in Chinese PRKAG2 cardiac syndrome. First, we have identified a novel heterozygous mutation, G100S in PRKAG2, which is present in all affected individuals in the family, but does not exist in another simple hypertrophic cardiomyopathy family and 100 controls. Second, we have confirmed that expression of PRKAG2 protein in CCL13 cells and subsequently, the G100S mutation reduces PRKAG2 protein expression. Third, we have demonstrated that the G100S mutation impairs PRKAG2-mediated activity of AMPK and leads to dysregulated glycogen metabolism in CCL13 cells. Fourth, the G100S mutation in non-CBS domains and the R302Q mutation in CBS domains result in similar functional consequences although resulting in different changes in PRKAG2 protein levels. To our knowledge, our findings represent not only the first mutation located in non-CBS domains of PRKAG2, but also the first description of the clinical and biochemical effects of non-CBS domains of PRKAG2.

The PRKAG2 gene has two different transcripts: PRKAG2-a, a full-length transcript and PRKAG2-b, a truncated transcript, which are composed of 16 and 12 exons and span 300 kb and 80 kb in length, respectively [3,21,22]. These two transcripts have four identical and consecutive CBS domains, a characteristic structure of AMPKγ2 subunit, which tandems to form the Bateman domain. The Bateman domain is highly conserved across species examined to date. By overexpressing PRKAG2 gene in CCL13 cells, John et al. demonstrated that the four tandem pairs of CBS domains in the γ subunits of AMPK form allosteric binding sites for adenosine derivatives and provide two allosteric binding sites for AMP and ATP [12]. Pathogenic mutations including R302Q, H383R, T400N, and R531G lead to an increase for binding of AMP to CBS domains of γ2. This reveals that tandem pairs of CBS domains play as a sensor of cellular energy status. However, the function of non-CBS domains is still unknown. One interesting feature is that the previous nine pathogenic mutations tend to occur in CBS domains, whereas the new mutation G100S is located in non-CBS domains. Our results show that G100S in non-CBS domains have similar but less mutational effects compared with R302Q in CBS domains. This suggests that the mechanism of G100S in non-CBS domains regulating AMPK activity may be consistent with that of R302Q in CBS domains. Our results support the idea that the function of non-CBS domains may be similar to CBS domains. Whether the mutation in non-CBS domains indirectly changes the binding ability of CBS domains to AMP and ATP is not clear. We speculate that either non-CBS domains have an ability of binding AMP and ATP or the mutation in this region that alters protein structure ultimately results in functional changes of CBS domains.

Our studies on AMPK activation or glycogen accumulation are in good agreement with previous studies [12–15], which show that mutations associated with hereditary diseases exhibit defective loss or decrease in AMPK activity. Consistent with our results, marked attenuation or absent enzymatic activity associated with the R302Q mutation *in vitro* has been reported. Furthermore, Scott et al. confirmed the mutation R302Q causing loss of enzymatic activity and revealed the mechanism to the decreased binding activity to AMP [23]. *In vivo* studies by Sidhu et al. show enzymatic activity of AMPK is significantly reduced, presumably owing to the mutation disrupting the AMP binding site, and excessive cardiac glycogen is observed in the TG_{R302Q} heart [14]. Further *in vivo* studies by Davies et al. proposed that the R531G mutation in γ2 leads to suppression of total cardiac AMPK activity secondary to the increased glycogen accumulation in transgenic mice [24]. These studies not only show that the primary defect of a mutant is caused by loss of AMPK activity and increased glycogen synthesis, but also suggest the molecular basis which provides insight into development of ventricular preexcitation, conduction defects, and cardiac hypertrophy. New evidence is added by our study that CCL13 cells show increased glycogen deposition resulting from the G100S and R302Q mutations.

Neither our results nor the above-mentioned studies [12–15] support the previous claim [3] that the N488I mutation is associated with increased AMPK activity. Nevertheless, the transgenic mice overexpressing the mutation N488I manifest the phenotype of large amounts of cardiac glycogen (30-fold above normal) accumulating, which provides an anatomic explanation for ventricular hypertrophy (because of *per se* glycogen accumulation) and ventricular preexcitation (because of disruption of the annulus fibrosis by glycogen-engorged myocytes). The authors suggest the mechanism of increased absorption of glucose. The effect of three mutations (R302Q, N488I, and R531G mutations) on AMPK activity remains controversial. Further *in vivo* studies [16] show that there is a biphasic response of AMPK activity to the T400N mutation in PRKAG2 in the TG_{T400N} murine model, providing an explanation for the discrepant findings concerning AMPK activity in previous studies.

An important subsidiary finding of our study was that the G100S and R302Q mutations did not cause increase of CCL13 cell apoptosis compared with WT PRKAG2 gene, in the presence or absence of AMPK activator—AICAR. In contrast, previous studies suggest that apoptosis could be induced by AMPK, which induces apoptosis of pancreatic β-cells though c-myc or c-Jun N-kinase and posticus caspase pathway, and apoptosis of neuroblastoma by caspase pathway, after activation by AICAR [25–27]. Our results indicate that AMPK, by some specified mechanism, may exert influence on the growth of a few phyletic cells, rather than all types of cells.

A second subsidiary finding from our study was that no influence of the G100S and R302Q mutations in PRKAG2 on intracellular location of PRKAG2 protein was observed, although the mutations impair AMPK activation. Taken together, our data strongly suggest that the role of the γ2 subunit regulating AMPK activity is not associated with the location of the protein in cells and indicate that the mutation of PRKAG2 does not affect the ability of permeating mesoplasts when expressed in CCL13 cells.

In summary, the novel missense mutation G100S in PRKAG2 may participate in the regulation of cells' vital movement through the AMPK signal pathway and is responsible for the Chinese PCS. The results also support the notion that PCS is a glycogen storage disease. Interestingly, Light et al. [28] suggest that cardiac voltage-gated sodium channels are regulated by overexpression of a constitutively active AMPK mutant and propose that sodium channels may be substrates of AMPK, possibly contributing to development of arrhythmia in PCS. Therefore, other distinct signal pathways may exist, which remains to be determined.

However, there still exist some limitations in our study. This experiment was performed to preliminarily explain the biological effect of PRKAG2 G100S mutation and further *in vivo* experiments should be carried out; we should further persuade the family members to obtain cardiac biopsy samples and detect the glycogen storage; a qualitative change in PRKAG2 protein should be further confirmed.

Acknowledgments

This work was supported in part by the National Natural Science Foundation (81000038) of China. We appreciate the administrative assistance of Professor Xiao-jing Ma in the preparation of this manuscript and figures. We also thank Dr Hua-mao Wang for providing the CCL13 cell lines.

References

[1] Hardie DG. Minireview: the AMP-activated protein kinase cascade: the key sensor of cellular energy status. Endocrinology 2003;144:5179–83.
[2] Blair E, Redwood C, Ashrafian H, Oliveira M, Broxholme J, Kerr B, Salmon A, Ostman-Smith I, Watkins H. Mutations in the gamma(2) subunit of AMP-activated protein kinase cause familial hypertrophic cardiomyopathy: evidence for the central role of energy compromise in disease pathogenesis. Hum Mol Genet 2001;10:1215–20.
[3] Gollob MH, Seger JJ, Gollob TN, Tapscott T, Gonzales O, Bachinski L, Roberts R. Novel PRKAG2 mutation responsible for the genetic syndrome of ventricular preexcitation and conduction system disease with childhood onset and absence of cardiac hypertrophy. Circulation 2001;104:3030–3.
[4] Gollob MH, Green MS, Tang AS, Gollob T, Karibe A, Ali Hassan AS, Ahmad F, Lozado R, Shah G, Fananapazir L, Bachinski LL, Roberts R. Identification of a gene responsible for familial Wolff–Parkinson–White syndrome. N Engl J Med 2001;344:1823–31.
[5] Arad M, Benson DW, Perez-Atayde AR, McKenna WJ, Sparks EA, Kanter RJ, McGarry K, Seidman JG, Seidman CE. Constitutively active AMP kinase mutations cause glycogen storage disease mimicking hypertrophic cardiomyopathy. J Clin Invest 2002;109:357–62.
[6] Arad M, Maron BJ, Gorham JM, Johnson WH, Saul JP, Perez-Atayde AR, Spirito P, Wright GB, Kanter RJ, Seidman CE, Seidman JG. Glycogen storage diseases presenting as hypertrophic cardiomyopathy. New Engl J Med 2005;352:362–72.
[7] Murphy RT, Mogensen J, McGarry K, Bahl A, Evans A, Osman E, Syrris P, Gorman G, Farrell M, Holton JL, Hanna MG, Hughes S, Elliott PM, Macrae CA, McKenna WJ. Adenosine monophosphate-activated protein kinase disease mimicks hypertrophic cardiomyopathy and Wolff–Parkinson–White syndrome: natural history. J Am Coll Cardiol 2005;45:922–30.
[8] Bayrak F, Komurcu-Bayrak E, Mutlu B, Kahveci G, Basaran Y, Erginel-Unaltuna N. Ventricular pre-excitation and cardiac hypertrophy mimicking hypertrophic cardiomyopathy in a Turkish family with a novel PRKAG2 mutation. Eur J Heart Fail 2006;8:712–5.
[9] Laforet P, Richard P, Said MA, Romero NB, Lacene E, Leroy JP, Baussan C, Hogrel JY, Lavergne T, Wahbi K, Hainque B, Duboc D. A new mutation in PRKAG2 gene causing hypertrophic cardiomyopathy with conduction system disease and muscular glycogenosis. Neuromuscul Disord 2006;16:178–82.
[10] Sternick EB, Oliva A, Magalh LP, Gerken LM, Hong K, Santana O, Brugada P, Brugada J, Brugada R. Familial pseudo-Wolff–Parkinson–White syndrome. J Cardiovascul lectrophysiol 2006;17:724–32.
[11] Arad M, Moskowitz IP, Patel VV, Ahmad F, Perez-Atayde AR, Sawyer DB, Walter M, Li GH, Burgon PG, Maguire CT, Stapleton D, Schmitt JP, Guo XX, Pizard A, Kupershmidt S, et al. Transgenic mice overexpressing mutant PRKAG2 define the cause of Wolff–Parkinson–White syndrome in glycogen storage cardiomyopathy. Circulation 2003;107:2850–6.
[12] Scott JW, Hawley SA, Green KA, Anis M, Stewart G, Scullion GA, Norman DG, Hardie DG. CBS domains form energy-sensing modules whose binding of adenosine ligands is disrupted by disease mutations. J Clin Invest 2004;113:274–84.
[13] Daniel T, Carling D. Functional analysis of mutations in the gamma 2 subunit of AMP-activated protein kinase associated with cardiac hypertrophy and Wolff–Parkinson–White syndrome. J Biol Chem 2002;277:51017–24.
[14] Sidhu JS, Rajawat YS, Rami TG, Gollob MH, Wang Z, Yuan R, Marian AJ, DeMayo FJ, Weilbacher D, Taffet GE, Davies JK, Carling D, Khoury DS, Roberts R. Transgenic mouse model of ventricular preexcitation and atrioventricular reentrant tachycardia induced by an AMP-activated protein kinase loss-of-function mutation responsible for Wolff–Parkinson–White syndrome. Circulation 2005;111:21–9.
[15] Davies JK, Wells DJ, Liu K, Whitrow HR, Daniel TD, Grignani R, Lygate CA, Schneider JE, Noel G, Watkins H, Carling D. Characterization of the role of gamma2 R531G mutation in AMP-activated protein kinase in cardiac hypertrophy and Wolff–Parkinson–White syndrome. Am J Physiol Heart Circ Physiol 2006;290:H1942–51.
[16] Banerjee SK, Ramani R, Saba S, Rager J, Tian R, Mathier MA, Ahmad F. A PRKAG2 mutation causes biphasic changes in myocardial AMPK activity and does not protect against ischemia. Biochem Biophy Res Commu 2007;360:381–7.
[17] Maron BJ, McKenna WJ, Danielson GK, Kappenberger LJ, Kuhn HJ, Seidman CE, Shah PM, Spencer III WH, Spirito P, Ten Cate FJ, Wigle ED. American College of Cardiology/European Society of Cardiology clinical expert consensus document on hypertrophic cardiomyopathy. A report of the American College of Cardiology Foundation Task Force on Clinical Expert Consensus Documents and the European Society of Cardiology Committee for Practice Guidelines. J Am Coll Cardiol 2003;42:1687–713.
[18] Goto D, Kinugawa S, Hamaguchi S, Sakakibara M, Tsuchihashi-Makaya M, Yokota T, Yamada S, Yokoshiki H, Tsutsui H. Clinical characteristics and outcomes of dilated phase of hypertrophic cardiomyopathy: report from the registry data in Japan. J Cardiol 2012.
[19] Nojiri A, Hongo K, Kawai M, Komukai K, Sakuma T, Taniguchi I, Yoshimura M. Scoring of late gadolinium enhancement in cardiac magnetic resonance imaging can predict cardiac events in patients with hypertrophic cardiomyopathy. J Cardiol 2011;58:253–60.
[20] Moon YJ, Lee MW, Yoon HH, Yang MS, Jang IK, Lee JE, Kim HE, Eom YW, Park JS, Kim HC, Kim YJ, Lee KH. Hepatic differentiation of cord blood-derived multipotent progenitor cells (MPCs) in vitro. Cell Biol Int 2008;32:1293–301.
[21] Cheung PCF, Salt IP, Davies SP, Hardie DG, Carling D. Characterization of AMP-activated protein kinase gamma-subunit isoforms and their role in AMP binding. Biochem J 2000;346:659–69.
[22] Lang TM, Yu L, Tu Q, Jiang JM, Chen Z, Xin YR, Liu GY, Zhao SY. Molecular cloning, genomic organization, and mapping of PRKAG2, a heart abundant gamma(2) subunit of 5′-AMP-activated protein kinase, to human chromosome 7q36. Genomics 2000;70:258–63.
[23] Scott JW, Green KA, Anis M, Stewart G, Scullion GA, Norman DG, Hardie DG. CBS domains form energy-sensing modules whose binding of adenosine ligands is disrupted by disease mutations. J Clin Invest 2004;113:274–84.
[24] Davies JK, Liu K, Whitrow HR, Daniel TD, Grignani R, Lygate CA, Schneider JE, Noël G, Watkins H, Carling D. Characterization of the role of gamma2 R531G mutation in AMP-activated protein kinase in cardiac hypertrophy and Wolff–Parkinson–White syndrome. Am J Physiol Heart Circ Physiol 2006;290:H1942–51.
[25] Kefas BA, Cai Y, Ling Z, Heimberg H, Hue L, Pipeleers D, Van de Casteele M. AMP-activated protein kinase can induce apoptosis of insulin-producing MIN6 cells through stimulation of c-Jun-N-terminal kinase. J Mol Endocrinol 2003;30:151–61.
[26] Van de Casteele M, Kefas BA, Cai Y, Heimberg H, Scott DK, Henquin JC, Pipeleers D, Jonas JC. Prolonged culture in low glucose induces apoptosis of rat pancreatic beta-cells through induction of c-myc. Biochem Biophy Res Commun 2003;12:937–44.
[27] Garcia-Gil M, Pesi R, Perna S, Allegrini S, Giannecchini M, Camici M, Tozzi MG. 5′-Aminoimidazole-4-carboxamide riboside induces apoptosis in human neuroblastoma cells. Neuroscience 2003;117:811–20.
[28] Light PE, Wallace CHR, Dyck JRB. Constitutively active adenosine monophosphate—activated protein kinase regulates voltage-gated sodium channels in ventricular myocytes. Circulation 2003;107:1962–5.